Nanoparticle Ferrite Multilayers Prepared by New Self-Assembling Sequential Adsorption Method

Yeong Il Kim,* Hojun Kang, Don Kim, and Choong Sub Lee*,†

Department of Chemistry, Pukyong National University, Pusan 608-737, Korea
†Department of Physics, Pukyong National University, Pusan 608-737, Korea
Received June 1, 2002

The nanoparticle magnetite of which diameter was about 3 nm was synthesized in a homogeneous aqueous solution without a template. The synthesized magnetite nanoparticle was easily oxidized to maghemite in an ambient condition. The magnetic properties of the ferrite nanoparticle show superparamagnetism at room temperature and its blocking temperature is around 93 K. Modifying the sequential adsorption method of metal bisphosphonate, we have prepared a multilayer thin film of the ferrite nanoparticle on planar substrates such as glass, quartz and Si wafer. In this multilayer the ferrite nanoparticle layer and an alkylbisphosphonate layer are alternately placed on the substrates by simple immersion in the solutions of the ferrite nanoparticle and 1, 10-decanediylbis (phosphonic acid) (DBPA), alternately. This is the first example, as far as we know, of nanoparticle/alkyl-bisphosphonate multilayer which is an analogy of metal bisphosphonate multilayer. UV-visible absorption and infrared reflection-absorption studies show that the growth of each layer is very systematic and the film is considerably optically transparent to visible light of 400-700 nm. Atomic force microscopic images of the film show that the surface morphology of the film follows that of the substrate in μm-scale image and the nanoparticle-terminated surface is differentiated from the DBPA-terminated one in nm-scale image. The magnetic properties of this ferrite/DBPA thin film are almost the same as those of the ferrite nanoparticle powder only.

Key Words : Magnetite, Nanoparticle, Metal bisphosphonate, Self-assembly

Introduction

The investigation and preparation of nanosized and nanostructured materials have recently become a very exciting area of fundamental and applied researches in chemistry and material sciences.[1] Since nanoparticles often have novel properties that are different from those of bulk materials due to their small size, they are becoming a core component of advanced materials that have wide practical applications with noble optical, electrical, magnetic, and catalytic properties.[2] Organic/inorganic hybrid thin film based on inorganic nanoparticles is one of stimulating nanostructured materials.[3] Layer-by-layer growth of nanoparticles is a very prospective strategy for preparing nanostructured thin films since it can give a fine control over the incorporated components and the thickness of film on a variety of surfaces.

There are some reported techniques for preparing nanoparticle-incorporated multiplayer thin fim which can be grown layer-by-layer: Langmuir-Blodgett(L-B) method,[4] polyelectrolyte method,[5] and alkyl dithiol method.[6] L-B method is the oldest and well-established multiplayer technique.[7] However this method requires a number of physical manipulations in order to transfer a layer preassembled by mechanical force to a substrate, and the prepared film is thermodynamically unstable. The polyelectrolyte and dithiol methods utilize self-assembly between a nanoparticle and a cross-link molecule. Among the self-assembling multiplayer techniques, there is a metal bisphosphonate multiplayer technique which is developed by Mallouk *et al*.[8] This multiplayer thin film is structurally very similar to L-B film but is thermodynamically more stable and mechanically robust than L-B film because the metal ions are chemically coordinated to interlayer cross linkers of bisphosphonates.

Recent reports showed that phosphonate derivatives were strongly adsorbed on the surface of metal oxide such as TiO_2 through the surface chelation of phosphonate.[9] Utilizing this surface chelation of phosphonate, it may be possible to stepwisely stack metal oxide nanoparticles using an alkyl bisphosphonate as an interlayer cross-linking agent as shown in gold nanoparticle multiplayer by the dithiol method.[6] In this case, metal oxide nanoparticles will replace metal ions in a metal bisphosphonate multiplayer. Therefore, we present here new layer-by-layer stacking method of inorganic metal oxide and organic alkyl chain utilizing the surface chelation of phosphonate functional group to metal oxide surface. For this study, we used magnetic nanoparticles since they are of great interest for wide practical applications[10] in information storage systems, catalyst, color imaging, ferrofluid, and medical diagnostics. First, We have synthesized and characterized magnetite nanoparticles in an aqueous solution.

Experimental Section

Materials. $FeCl_2 \cdot 4H_2O$ (99%), $FeCl_3 \cdot 6H_2O$ (98%), 1,10-

*To whom correspondence should be addressed. e-mail: ykim@pknu.ac.kr (Yeoung I1 Kim); cslee@pknu.ac.kr (Choong Sub Lee)

dibromodecane (97%), zirconyl chloride (98%), and 2,6-lutidine were purchased from Aldrich. triethyl phosphite (97%) and phosphorous oxychloride (98%) were obtained from Fluka. 1,10-decanediylbisphosphonic acid (DBPA) was synthesized by Michaelis-Arbuzov reaction of Br $(CH_2)_{10}Br$ and $P(OCH_2H_5)_3$ as a literature method.[8b] 4-mercaptobutanephosphonic acid (MBPA) was obtained from Prof. Taisun Kim, Hallim University who synthesized it by a literature method.[11] Slide glass, quartz plate and Si-wafer(n-type, 111) were obtained from Menzel-Glaser, GM glass and Wafernet, respectively. Au substrate of about 2000 Å thickness was prepared by thermal evaporation on Si-wafer with Cr-subcoating. All substrates were cleaned in Piranha solution ($98\%H_2SO_4 : 30\%H_2O_2 = 3 : 1$ v/v) for 10 min and washed with a copious amount of water and dried in a vacuum oven at 50 °C. Acetonitrile was dried by distillation in P_2O_5 before use. Deionized water was obtained from Barnstead Nanopure system and was used in all experiemnts.

Apparatus. X-ray diffraction patterns were measured by Rigagu D/Max-2400 X-ray diffractometer with CuKα source and 0.01°/sec scan rate. Transmission electron micrograph (TEM) and scanning electron micrograph (SEM) were taken with Jeol JFM 2000fxII and Hitachi U-4200, respectively. The infrared reflection-absorption spectra were measured by Perkin-Elmer Spectrum 2000 with a variable angle specular reflectance accessory and a MCT detector. The data were recorded in reflection mode operating with approximately 83° incident angle and with averaging 2000 scans. Atomic force microscopic (AFM) images were taken by Park Science Instrument Autoprobe CP in contact mode with a commercial Si_3N_4 cantilever of 0.05 N/m force constant. Temperature dependence of magnetization was measured with Lakeshore 7000 ac-magnetic susceptometer at 1 Oe, 125 Hz. Magnetizations as a function of applied magnetic field were measured with Lakeshore 7300 vibrating sample magnetometer and Quantum Design MPMS 7 SQUID magnetometer for powder sample and thin film, respectively.

Preparation of Ferrite Nanoparticle and Ferrite/DBPA Multilayer. The synthetic procedure of nanoparticle magnetite was reported in the previous paper.[12] The only difference is that the synthesis was done in a refrigerated circulating bath at 0 °C. The wet magnetite slurry immediately after synthesis was suspended in water adjusted to pH 4. It was sonicated for 20 min and centrifuged at 10000 rpm. The resulting colloidal solution was very stable for several months and used for the multilayer film. In order to prepare magnetite/DBPA multiplayer film, all substrates such as glass, quartz, and Si wafer were first pretreated by being dipped in an anhydrous acetonitrile solution of both 10 mM $POCl_3$ and 2,6-lutidine for an hour, then rinsed with acetonitrile and water and dipped in 20 mM $ZrOCl_2$ aqueous solution for 30 min. Magnetite/DBPA multiplayer was grown layer-by-layer on the substrates by repeating alternate dipping in 5 mM DBPA methanol solution and the magnetite colloidal solution as shown in Scheme 1. The substrate was thoroughly washed with a copious amount of water between immersions. For IR reflection-absorption measurement, Au-coated Si wafer and 4-mercaptobutanephosphonic acid were used as a substrate and a surface-anchoring compound, respectively.[5d,8]

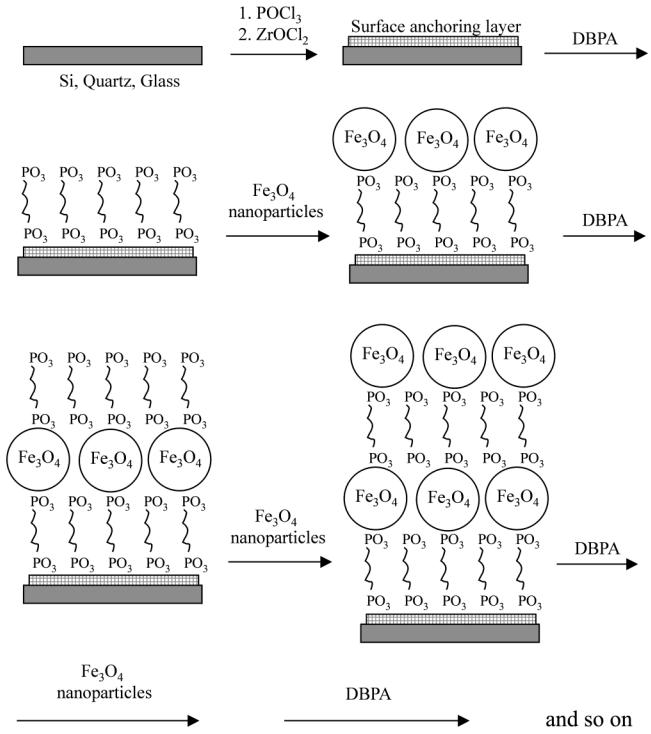

Scheme 1. Schematic representation of preparing ferrite-nanoparticle/DBPA multilayer by the self-assembling sequential adsorption method.

Results and Discussion

Characterization of Synthesized Magnetite Nanoparticle. Figure 1(a) shows the XRD pattern of nanoparticle magnetite which was prepared in an aqueous solution at 0 °C. The data were corrected with background subtraction and smoothed because the signal-to-nose ratio was low due

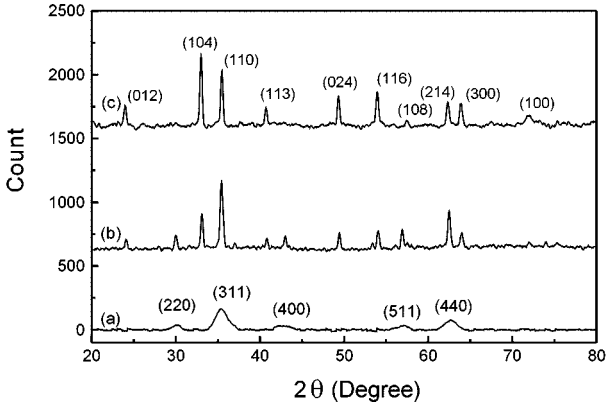

Figure 1. XRD pattern of the synthesized ferrites: (a) as is right after synthesis, (b) the annealed one under vacuum at 500 °C for 1 hour right after synthesis and (c) the annealed one which had been exposed to air for 2 weeks after synthesis, under vacuum at 500 °C for 1 hour.

to the small size and poor crystallinity. The peaks are nearly same to those of the structure of magnetite or maghemite.[13] It is difficult to distinguish magnetite from maghemite by the XRD pattern because they have the same inverse-spinnel structure and are isomorphic. The unit cell parameter was estimated to be 8.381 using Nelson-Riley extrapolation. This value lies between those of magnetite (8.396) and maghemite (8.35).[14] In the previous study,[15] we have shown that magnetite nanoparticle of which diameter is about 7 nm was transformed to maghemite in an ambient condition (air, room temperature). It is expected that the magnetite nanoparticle prepared here will be transformed more easily to maghemite than the nanoparticle of 7 nm in diameter did due to its smaller particle size. Since the change of XRD pattern is not discernible before and after transformation, we have sealed the sample in a quartz tube under vacuum and annealed it at 500 °C for an hour as discussed in the previous study.[15] Figure 1(b) and 1(c) are the XRD patterns of the annealed one right after synthesis and after having been exposed in air for 2 weeks, respectively. While the annealing of magnetite under vacuum at 500 °C gives no phase transformation, the annealing of maghemite in the same condition will cause the transformation of it to hematite. Figure 1(b) shows the XRD pattern of the mixture of magnetite and hematite for the annealed sample that was sealed in vacuum right after synthesis. Figure 1(c) shows the pattern of only hematite for the sample that had been exposed to air for 2 week after synthesis and been annealed. Therefore, the nanoparticle ferrite was consisted of the mixture of magnetite and maghemite right after synthesis and the magnetite was entirely oxidized to maghemite in 2 weeks when it was exposed to air. Although the synthesized ferrite is apparently the mixture of magnetite and maghemite, it might be in only magnetite phase immediately after it was prepared in the reaction solution because the air-exposure for sample preparation process such as centrifugation could not be completely prevented. The estimated particle size of the ferrite was 2.4 nm in diameter from (311) peak of Figure 1(a) by Debye-Scherrer equation.[16]

Figure 2 shows TEM picture of the synthesized ferrite nanoparticle. The shape of particles is round and the sizes are relatively homogeneous. The estimated average diameter is about 3 nm from 65 particles in the picture. This value is consistent with the value from XRD peak. This is less than half size of the one previously synthesized with the same method at room temperature.[15] Although many researchers have reported the synthesis of the nanoparticle magnetite or maghemite whose diameter is smaller than 5 nm,[17] most of them were synthesized in some templates or matrixes such as sol-gel,[17d] micelle,[17c] microemulsion,[17a,e] polymers,[17f] block copolymer,[17b] and aluminosilicate.[17g] In our case, we have synthesized magnetite/maghemite ferrite[18] whose size is as small as about 3 nm in diameter in an aqueous homogeneous solution by simply lowering preparation temperature.[19]

The magnetization of the nanoparticle ferrite powder as a function of applied magnetic field is shown in Figure 3. Although bulk maghemite and magnetite are ferrimagnetic at room temperature, there is no magnetic hysteresis at room temperature for this ferrite. This is characteristic of superparamagnetic nanopaticles where thermal fluctuations are sufficient to overcome the anisotropy energy barrier.[20] The magnetic moment at the maximum applied field (18 kOe) is about 28 emu/g. This value is about one third of that of the saturation magnetization of bulk magnetite, 76 emu/g.[21] In the case of single-domain superparamagnetic particles with a finite size, the relationship between magnetization (M) and applied field (H) at a specific temperature can be described by Langevin function.[21] Neglecting a size distribution of the nanoaprticles, fitting of M-H data to Langevin function can give a rough estimation of the size of the ferrite. In this way we obtained the diameter of the ferrite nanoparticle as about 3 nm from the fitting of Figure 3. This result is very consistent with those of TEM and XRD.

Figure 4 shows the temperature dependence of ac magnetic susceptibility(dM/dH) for the ferrite powder. Ac magnetic susceptibility is measured in a small oscillating magnetic field without static magnetic field and gives almost the same information as zero-field-cooled data of dc magnetic susceptibility(M/H) measured in weak magnetic field. As a temperature decreased, the susceptibility increased until it reached at the maximum at 93 K and then decreased. The decrease at low temperature is due to the freezing of

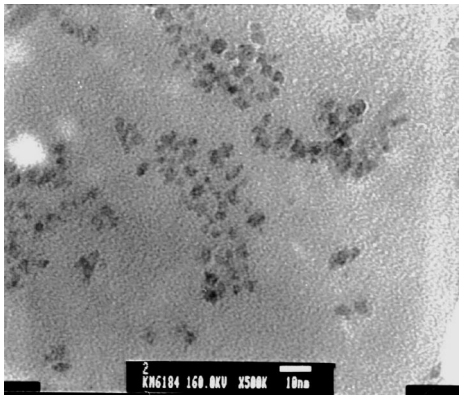

Figure 2. TEM picture of the synthesized ferrite nanoparticle (scale bar: 10 nm).

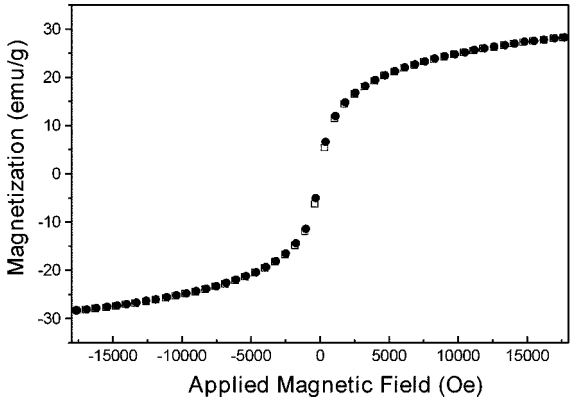

Figure 3. Magnetization *vs* applied magnetic field for the powder of synthesized ferrite nanoparticles at room temperature.

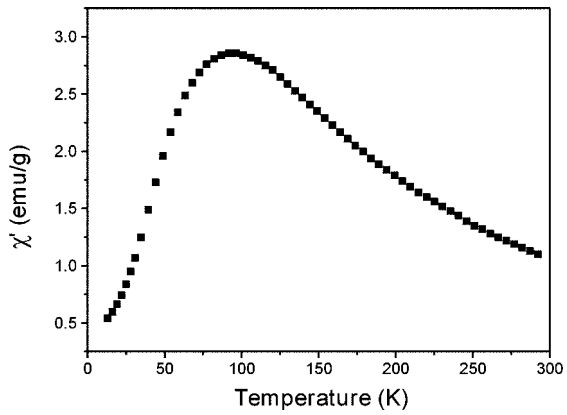

Figure 4. Temperature-dependent ac magnetic susceptibility for the powder of synthesized ferrite nanoparticles (in-phase component, χ')

disordered spin system and is usually known in the materials of mictomagnetism and spin glass.[22] It is also well known in superparamagnetic nanoparticles because the total magnetic moment is frozen in the process of random agitation by thermal fluctuation. The temperature at a maximum susceptibility (T_{max}) is related to a blocking temperature (T_B) which is a boundary temperature between ferromagnetism and superparamagnetism. T_B can be experimentally determined from the temperature where a zero-field-cooled data begins to match with a field-cooled data in dc magnetic susceptibility measurement or where a magnetic hyperfine interaction starts to appear in Mösbauer spectrum.[23] If the particle size is uniform, T_{max} corresponds to T_B because the splitting of zero-field-cooled data and field-cooled data start at the maximum susceptibility. In the sample with a wide size distribution, the splitting starts at a temperature higher than T_{max} and the temperature corresponds to T_B of the largest particles in the sample. T_{max} corresponds to average blocking temperature of whole sample.[17e] From the data of Figure 4, we can estimate the average blocking temperature of the synthesized nanoapticle ferrite powder as 93 K. This value of T_B is relatively higher than those reported for nanoparticle maghemites which were synthesized in a similar size with some templates.[17b,d]

Nanoparticle-Ferrite/DBPA Complex Multilayer. As shown in Scheme 1, we constructed organic/inorganic composite multilayer by stacking DBPA layer and ferrite nanoparticle layer alternately. The driving force of layer stacking is the strong adsorption of phosphonnate to the surface of metal oxide as mentioned in Introduction. The surface anchoring to the substrates such as glass, quartz, and Si wafer which have hyroxyl group on its surface was done by a direct phosphorylation with $POCl_3$ and a subsequent zirconation with $ZrOCl_2$ without using anchoring aminosilane compound Katz *et al.* used.[24] This initial anchoring step was not so critical that DBPA molecule could be directly adsorbed on the substrates as reported in our other study.[25] Only the surface coverage in the case of without anchoring step was slightly lower than that with the step.

UV-Vis absorption spectra of the ferrite/DBPA multiplayer on a quartz plate are shown in Figure 5. The absorption is

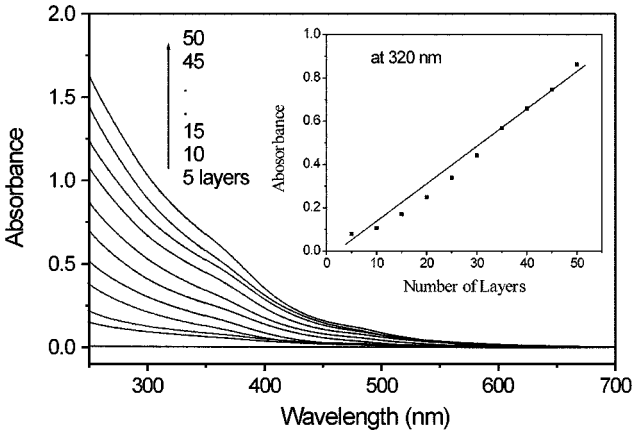

Figure 5. UV-Vis absorption spectra of the ferrite/DBPA multiplayer on a quartz substrate. The inset shows the absorbance *vs* number of layers at 320 nm.

due to only ferrite nanoparticles since DBPA does not absorb visible light. The feature of absorption spectrum is the same as that of the colloidal solution of the nanoparticle ferrite (not shown here). The multiplayer film is considerably transparent for visible light compared with bulk maghemite due to the size quantization effect.[26] As shown in the inset graph, the absorption linearly increases as the number of layer increases. This means that the amount of the nanoparticle ferrites included in each layer is somewhat uniform.

In order to confirm the systematic increment of DBPA layer, we measured infrared reflection-absorption spectra of ferrite/DBPA multiplayers. The layers were deposited on gold surface on Si-wafer using MBPA as an anchoring agent. Figure 6 shows IR absorption bands of CH_2-stretching vibration in the multiplayer. The absorption peaks appear at 2925-2931 (ν_{as}) and 2852 (ν_s) cm^{-1}, which correspond to asymmetric and symmetric stretching, respectively. The inset shows that the integrated peak-areas increased relatively linearly as the number of layer increased. Therefore DBPA layer also systematically increases as well as the layer of

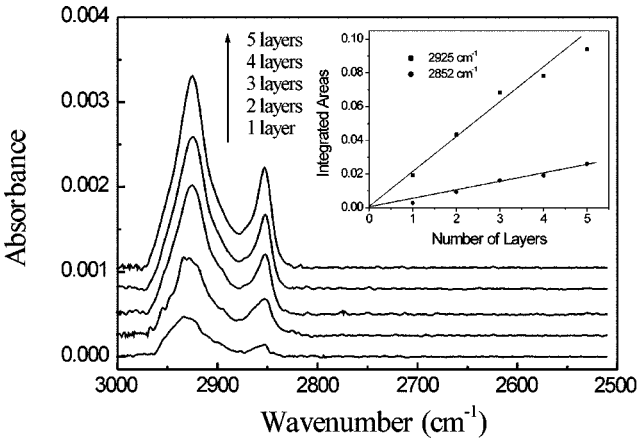

Figure 6. Reflection-absorption IR spectra of the ferrite/DBPA layers on a gold substrate. The inset shows the integrated peak area *vs* number of layers.

nanoparticles do as shown in UV-Vis absorption. The peak position and widths (about 40 and 20 cm^{-1} at ν_{as} and ν_s, respectively) are almost coincident with those of Zr-DBPA multiplayer film (41 and 23 cm^{-1} at 2929 (ν_{as}) and 2854 (ν_s) cm^{-1}, respectively).[8d] Since the peak position and width did not change appreciably as a new layer added, the degree of ordering of each layer may be relatively constant. The comparison of these data with a polycrystalline and an amorphous-like Zr-DBPA[8d] show that the structural ordering of DBPA in ferrite/DBPA multiplayer is pretty close to that in Zr-DBPA multiplayer.

The surface morphologies of ferrite/DBPA multiplayer were investigated by AFM. Figure 7 shows AFM images of bare slide glass and 5-layer ferrite/DBPA film. The deposition of film does not result in drastic morphology change on the glass substrate. The surface of bare slide glass looks consisted of round particles of 0.1-0.15 μm in diameter. However, the height difference is relatively small as maximum 12 nm. When the 5 layers of ferrite/DBPA were deposited, the particle-like surface was simply increased in diameter and the depth also slightly increased. A root-mean-squared roughness of bare glass and the film were 21 and 38 Å, respectively. Figure 8 shows AFM images of DBPA- and nanoparticle-terminated surfaces in nm scale. In this case, the multilayer was constructed on the surface of Si-wafer in order to confirm the flatness of substrate surface. The repeated measurements of different regions in one sample and a few samples gave relatively a consistent result. While the surface is smooth and flat when it is terminated with DBPA, the image of the surface shows hills and valleys and looks consisted of small particles of 2-3 nm in diameter when terminated with ferrite nanoparticles. Therefore, a stepwise construction of DBPA layer and nanoparticle layer, which is not randomly mixed together, was clearly seen. Figure 9 shows a SEM picture of side-cut view of the DBPA/ferrite 50-layer film on glass substrate. Although the picture is not so good, the multiplayer is clearly differentiated from the substrate. The thickness of the film is fairly uniform and is estimated as about 280 nm. The average thickness of each layer (DBPA + ferrite) can be estimated as about 5-6 nm. It can be concluded that each layer is consisted of the single particle and the single DBPA layers since the length of DBPA is roughly 2 nm[27] and the diameter of a ferrite

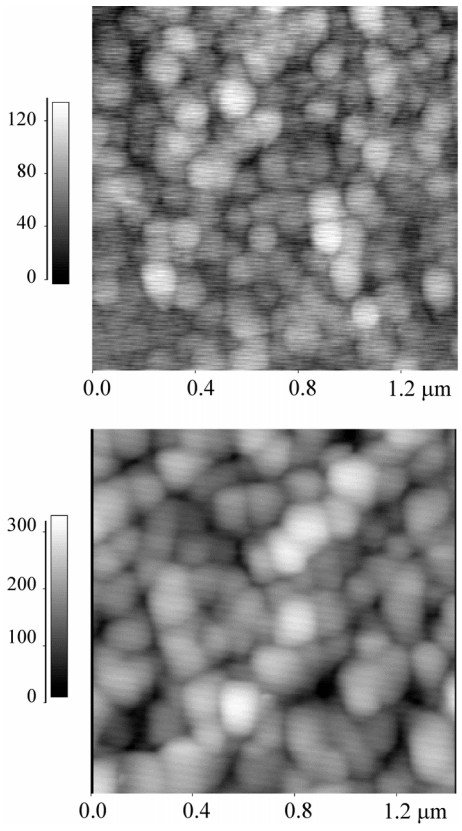

Figure 7. AFM images of the ferrite/DBPA layers on a glass substrate (top: bare glass substrate, bottom: after deposition of ferrite/DBPA 5 layers).

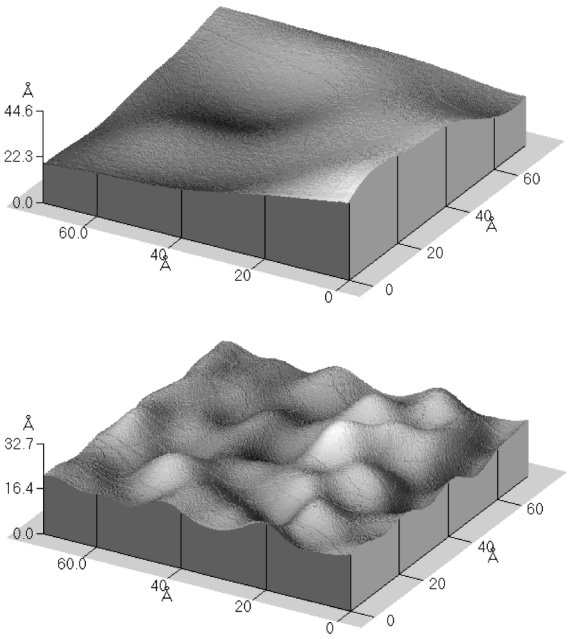

Figure 8. AFM images of 20 layers of the ferrite/DBPA on Si wafer (top: the surface was terminated with DBPA, bottom: terminated with ferrite nanoparticles)

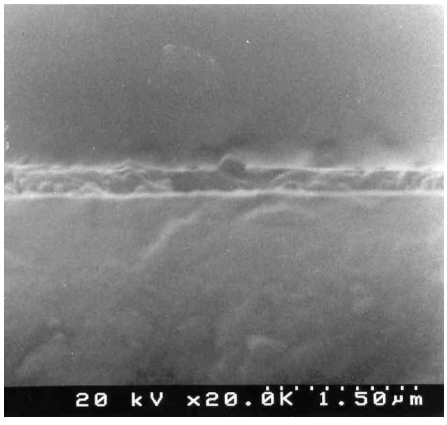

Figure 9. Side-cut view of SEM images of the ferrite/DBPA 50 layers on a glass substrate (scale bar: 1.5 μm).

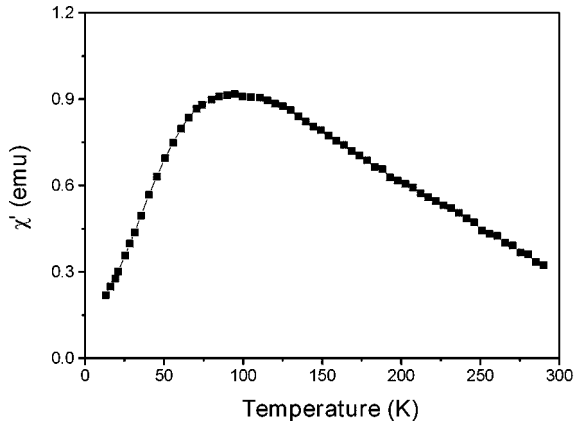

Figure 10. Temperature dependent ac magnetic susceptibility for the ferrite/DBPA multiplayer on glass substrate. (100 layers of ferrite/DBPA were scraped off from glass substrate for the measurement).

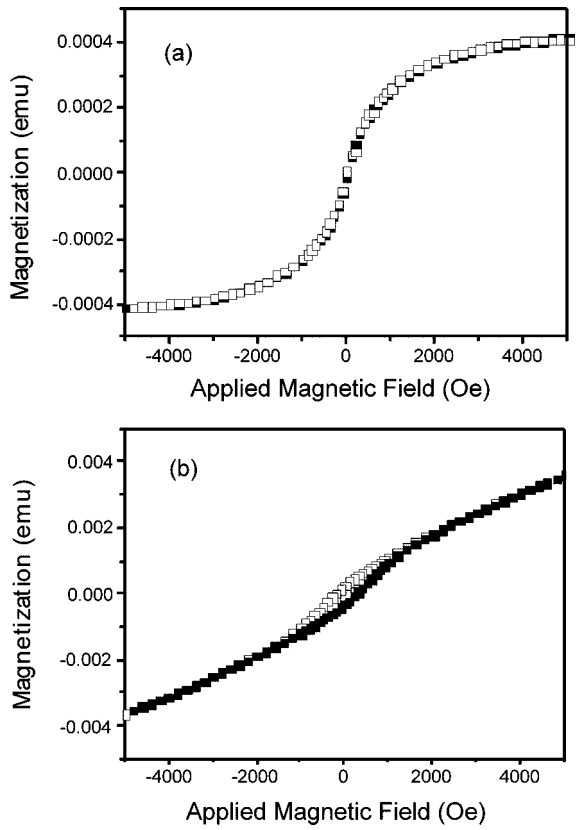

Figure 11. Magnetization vs. applied magnetic field for the ferrite/DBPA multiplayer on glass substrate at room temperature (100 layers, (a) at 300 K, (b) at 2 K).

nanoparticle is about 3 nm.

The magnetic properties of the ferrite/DBPA multiplayer film were investigated with the measurements of magnetization vs. applied magnetic field and temperature dependence of ac magnetic susceptibility. Figure 10 shows the temperature dependence of ac magnetic susceptibility for the 100 layers of ferrite/DBPA prepared on slide glass. The sample film used here was scraped off from the substrate with a doctor blade due to a difficulty of measurement. Figure 11 shows the changes of magnetization as a function of applied field for the same sample that is not scraped off, which is measured at 300 K and 2 K with SQUID magnetometer. The results are almost the same as those of nanoparticle ferrite powder shown in Figure 3 and 4. As discussed in previous section, the ferrite/DBPA film is also superparamagnetic at room temperature and its blocking temperature is about 90 K. Small hystereris appeared on the plot of magnetization vs applied field at the temperature of 2 K which is below the blocking temperature. At this temperature, the film became ferrimagnetic with coercivity of 240 Oe.

Conclusion

Ferrite-nanoparticle/alkyl-bisphosphonate complex multiplayer was prepared by self-assembling sequential adsorption method which is an analogy of metal bisphosphonate multiplayer. In this method, the coordination between metal ions and phosphonates was replaced with the adsorption of alkyl bisphosphonate to the surface of metal oxide. The multilayer could be grown up to more than 100 layers by simple alternate dips in the constituent solutions at an ambient condition. The data of UV-Vis and IR absorption and AFM and SEM pictures confirm that the growth of multilayer was very systematic. Each repeating unit layer was consisted of almost single nanoparticle layer and DBPA layer. The multiplayer film was mechanically robust and stable. The magnetic properties of the film are same to those of the nanoparticle ferrite powder which is superparamagnetic at room temperature. Since a phosphonic-acid derivative can be strongly adsorbed on the surfaces of most of metal oxides, this multiplayer technique can be easily applied to most of metal-oxide nanoparticles. We are now investigating the complex multiplayer of semiconducting nanoparticles such as TiO_2 and SnO_2.

Acknowledgement. This work was supported by Basic Science Research Institution Program of Ministry of Education (BSRI-97-2455) and Korea Research Foundation Grant (KRF-2000-015-DP0298). The authors thank Professor Taisun Kim (Hallym University) for providing us with 4-mercaptobutanephosphonic acid.

References

1. Fendler, J. H. *Nanoparticles and Nanostructured Films: Preparation, Characterization and Applications*; Wiley-VCH: Weinhein, 1998.
2. Henglein, A. *Chem. Rev.* **1989**, *89*, 1861. (b) Hagfeldt, A.; Grätzel, M. *Chem. Rev.* **1995**, *95*, 49. (c) Alivisatos, A. P. *Science* **1996**, *271*, 933. (c) *Nanoaprticles in Solids and Solutions*; Fendler, J. H.; Dékány, I., Ed.; Kluwer Academic: Dordrecht, 1996.
3. Adair, J. H.; Li, T.; Kido, T.; Havey, K.; Moon, J.; Mecholsky, J.; Morrone, A.; Talham, D. R.; Ludwig, M. H.; Wang, L. *Mater. Sci. Eng. R* **1998**, *R23*, 139.
4. (a) Yang, J.; Peng, X.-G.; Zhang, Y.; Wang, H.; Li, T.- J. *J. Phys. Chem.* **1993**, *97*, 4484. (b) Meldrum, F. C.; Kotov, N. A.; Fendler,

J. H. *J. Phys. Chem.* **1994**, *98*, 4506. (c) Nakaya, T.; Li, Y.-J.; Shibata, K. *J. Mater. Chem.* **1996**, *6*, 691. (d) Kang, Y. S.; Lee, D. K.; Stroeve, P. *Thin Solid Film*. **1998**, *327-329*, 541.
5. (a) Cassagneau, T.; Fendler, J. H. *J. Phys. Chem. B* **1999**, *103*, 1789. (b) Caruso, F.; Spasova, M.; Susha, A.; Giersig, M.; Caruso, R. A. *Chem. Mater.* **2001**, *13*, 109. (c) Gittins, D. I.; Susha, A. S.; Schoeler, B.; Caruso, F. *Adv. Mater.* **2002**, *14*, 508. (d) Dai, J.; Bruening, M. L. *Nano Lett.* **2002**, *2*, 497.
6. (a) Brust, M.; Etchenique, E. J.; Gordillo, G. J. *Chem. Commun.* **1996**, 1950. (b) Musick, M. D.; Keating, C. D.; Keefe, M. H.; Nathan, M. J. *Chem. Mater.* **1997**, *9*, 1499. (c) Nakanishi, T.; Ohtani, B.; Uosaki, K. *J. Phys. Chem*. **1998**, *102*, 1571. (d) Hu, K.; Brust, M.; Bard, A. J. *Chem. Mater.* **1998**, *10*, 1160. (e) Brust, M.; Bethell, D.; Kiely, C. J.; Shiffrin, D. J. *Langmuir* **1998**, *14*, 5425. (f) Sarathy, V. K.; Thomas, P. J.; Kulkarni, G. U.; Rao, C. N. R. *J. Phys. Chem.* **1999**, *103*, 399.
7. Gaines Jr., G. L. *Insoluble Monolayers at Liquid-Gas Interfaces*; Wiley Interscience: New York, 1966.
8. (a) Lee, H.; Kepley, L. J.; Hong, H.-G.; Mallouk, T. E. *J. Am. Chem. Soc*. **1988**, *110*, 618. (b) Lee, H.; Kepley, L. J.; Hong, H.-G.; Akhter, S.; Mallouk, T. E. *J. Phys. Chem*. **1988**, *92*, 2597. (c) Hong, H.-G.; Sackett, D. D.; Mallouk, T. E. *Chem. Mater.* **1991**, *3*, 521. (d) Yang, H. C.; Aoki, K.; Hong, H.-G.; Sackett, D. D.; Arendt, M. F.; Yau, S.-L.; Bell, C. M.; Mallouk, T. E. *J. Am. Chem. Soc*. **1993**, *115*, 11855.
9. (a) Pechy, P.; Rotzinger, F. P.; Nazeeruddin, M. K.; Kohle, O.; Zakeeruddin, S. M.; Humphry-Baker, R.; Grätzel, M. *J. Chem. Soc., Chem. Commun.* **1995**, 65. (b) Yan, S. G.; Hupp, J. T. *J. Phys. Chem.* **1996**, *100*, 6867. (c) Trammell, S. A.; Wimbish, J. C.; Odobel, F.; Gallagher, L. A.; Narula, P. M.; Meyer, T. J. *J. Am. Chem. Soc*. **1998**, *120*, 13248. (d) Lee, M. S.; Shim, H. K.; Kim, Y. I. *Mol. Cryst. Liq. Cryst.* **1998**, *316*, 401.
10. *Science and Technology of Nanostructured Magnetic Materials*; Hadjipanayis, G. C.; Prinz, G. A., Eds.; Plenum: New York, 1991.
11. Hong, H.-G.; Mallouk, T. E. *Langmuir* **1991**, *7*, 2362.
12. Kang, H.; Lee, C. S.; Kim, D.; Kang, Y. S.; Kim, Y. I. *Bull. Korean Chem. Soc*. **1998**, *19*, 408.
13. Cornell, R. M.; Schwertmann, U. *The Iron Oxides*; VCH: New York, 1996; p 167.
14. JCPDS (Joint Committee on Powder Diffraction Standards) data base 19-629 and 39-1246.
15. Kang, H.; Lee, C. S.; Kim, D.; Kang, Y. S.; Kim, Y. I. *Bull. Korean Chem. Soc*. **1998**, *19*, 408.
16. Azariff, L. B. *The Powder Method*; McGraw Hill: New York, 1958.
17. (a) Kommareddi, N. S.; Tata, M.; John, V. T.; McPherson, G. L.; Herman, M. F.; Lee, Y. S.; OConnor, J.; Akkara, J. A.; Kaplan, D. L. *Chem. Mater.* **1996**, *8*, 801. (b) Sohn, B. H.; Cohen, R. E. *Chem. Mater.* **1997**, *9*, 264. (c) Feltin, N.; Pileni, M. P. *Langmuir* **1997**, *13*, 3927. (d) Zhang, L.; Papaefthymiou, G. C.; Ying, J. Y. *J. Appl. Phys.* **1997**, *81*, 6892. (e) López Pérez, J. A.; López Quintela, M. A.; Mira, J.; Rivas, J.; Charles, S. W. *J. Phys. Chem. B* **1997**, *101*, 8045. (f) Pardope, H.; Chua-anusorn, W.; St. Pierre, T. G.; Dobson, J. *J. Magn. Magn. Mater.* **2001**, *225*, 41. (g) Zhang, L.; Papaefthymiou, G. C.; Ying, J. Y.; *J. Phys. Chem. B* **2001**, *105*, 7414. (h) Hyeon, T.; Lee, S. S.; Park, J.; Chung, Y.; Na, H. B. *J. Am. Chem. Soc*. **2001**, *123*, 12798. (i) Yadong, Y. L.; Mayers, B. T.; Xia, Y. *Nano Lett*. **2002**, *2*, 183.
18. We call the magnetic nanoparticle as simply “ferrite” in the rest discussion, since the nanopaticle was consisted of both magnetite and maghemite by partial transformation.
19. The manuscript of a temperature-controlled synthesis of nanoparticle magnetite and characterization of their magnetic properties is in preparation.
20. Gunther, L. In *Magnetic Properties of Fine Particles*; Dormann, J. L.; Fiorani, D., Eds.; Wiley: New York, 1992; p 213.
21. Cullity, B. D. In *Introduction to Magnetic Materials*; Addison-Wesley: Reading, MA, 1972; p 201.
22. Chikazumi, S. *Physics of Ferromagnetism*; Clarendon Press: Oxford, 1997; p 153.
23. Chien, C. L. In *Science and Technology of Nanostructured Magnetic Materials*; Hajipanayis, G. C.; Prinz, G. A., Eds.; Plenum Press: New York, 1991; p 477.
24. (a) Katz, H. E.; Scheller, G.; Putvinski, T. M.; Schilling, M. L.; Wilson, W. L.; Chidsey, C. E. D. *Science* **1991**, *254*, 1485. (b) Katz, H. E.; Schilling, M. L.; Chidsey, C. E. D.; Putvinski, T. M.; Hutton, R. S. *Chem. Mater.* **1991**, *3*, 699. (c) Ungashe, S. B.; Wilson, W. L.; Katz, H. E.; Scheller, G. R.; Putvinski, T. M. *J. Am. Chem. Soc*. **1992**, *114*, 8717. (d) Katz, H. E.; Schilling, M. L. *Chem. Mater.* **1993**, *5*, 1162. (e) Katz, H. E. *Chem. Mater*. **1994**, *6*, 2227. (f) Xu, X.-H.; Yang, H. C.; Mallouk, T. E.; Bard, A. J. *J. Am. Chem. Soc*. **1994**, *116*, 8386. (g) Vermeulen, L. A.; Thompson, M. E. *Nature* **1992**, *358*, 656. (h) Chae, H. J.; Lee, M. S.; Kim, Y. I.; Lee, H. *Bull. Korean Chem. Soc*. **1998**, *19*, 27. (i) Lee, M. S.; Shim, H. K.; Kim, Y. I. *Mol. Cryst. Liq. Cryst*. **1998**, *316*, 179.
25. Cho, K. J.; Shim, H. K.; Kim, Y. I. *Syn. Metals* **2001**, *117*, 153.
26. Ziolo, R. F.; Giannelis, E. P.; Weinstein, B. A.; OHoreo, M. P.; Ganguly, B. N.; Mehrotra, V.; Russell, M. W.; Huffman, D. R. *Science* **1992**, *257*, 219.
27. Since Zr-DBPA has 17.3 Å of crystallographic layer spacing in a tilted structure,[28] we have roughly assumed it.
28. Dines, M. B.; DiGiacomo, P. M. *Inorg. Chem.* **1981**, *20*, 92.